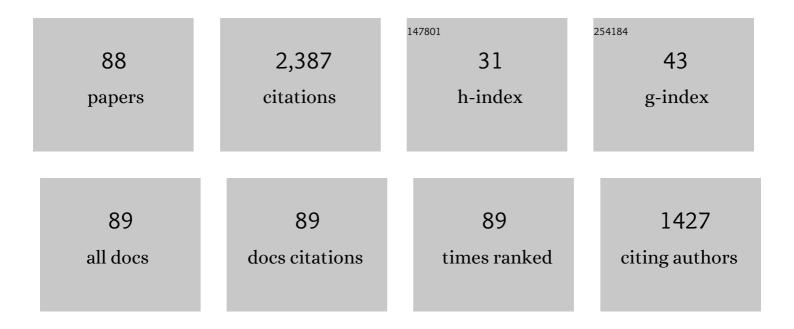
Nathan Daczko

List of Publications by Year in descending order

Source: https://exaly.com/author-pdf/4185164/publications.pdf Version: 2024-02-01



ΝΑΤΗΛΝ ΠΑΟΖΚΟ

#	Article	IF	CITATIONS
1	Cretaceous high-P granulites at Milford Sound, New Zealand: metamorphic history and emplacement in a convergent margin setting. Journal of Metamorphic Geology, 2000, 18, 359-374.	3.4	96
2	Decoding near-concordant U–Pb zircon ages spanning several hundred million years: recrystallisation, metamictisation or diffusion?. Contributions To Mineralogy and Petrology, 2012, 163, 67-85.	3.1	86
3	Transformation of two-pyroxene hornblende granulite to garnet granulite involving simultaneous melting and fracturing of the lower crust, Fiordland, New Zealand. Journal of Metamorphic Geology, 2001, 19, 549-562.	3.4	67
4	Kinematic vorticity and tectonic significance of superposed mylonites in a major lower crustal shear zone, northern Fiordland, New Zealand. Journal of Structural Geology, 1999, 21, 1385-1405.	2.3	66
5	Evidence of Early Cretaceous collisional-style orogenesis in northern Fiordland, New Zealand and its effects on the evolution of the lower crust. Journal of Structural Geology, 2001, 23, 693-713.	2.3	63
6	Plutonic rocks of Western Fiordland, New Zealand: Field relations, geochemistry, correlation, and nomenclature. New Zealand Journal of Geology, and Geophysics, 2009, 52, 379-415.	1.8	63
7	A method for applying matrix corrections to Xâ€ray intensity maps using the Bence–Albee algorithm and Matlab. Journal of Metamorphic Geology, 2001, 19, 635-644.	3.4	61
8	Geochronology and geochemistry of highâ€pressure granulites of the Arthur River Complex, Fiordland, New Zealand: Cretaceous magmatism and metamorphism on the palaeoâ€Pacific Margin. Journal of Metamorphic Geology, 2003, 21, 299-313.	3.4	60
9	Kyanite-paragonite-bearing assemblages, northern Fiordland, New Zealand: rapid cooling of the lower crustal root to a Cretaceous magmatic arc. Journal of Metamorphic Geology, 2002, 20, 887-902.	3.4	59
10	The regional significance of Cretaceous magmatism and metamorphism in Fiordland, New Zealand, from U-Pb zircon geochronology. Journal of Metamorphic Geology, 2004, 22, 607-627.	3.4	59
11	Mineral Equilibria Modeling of the Granulite–Eclogite Transition: Effects of Whole-Rock Composition on Metamorphic Facies Type-Assemblages. Journal of Petrology, 2012, 53, 949-970.	2.8	58
12	Thermal gradient and timing of highâ€ <i>T</i> –lowâ€ <i>P</i> metamorphism in the Wongwibinda Metamorphic Complex, southern New England Orogen, Australia. Journal of Metamorphic Geology, 2012, 30, 3-20.	3.4	46
13	A cryptic Gondwana-forming orogen located in Antarctica. Scientific Reports, 2018, 8, 8371.	3.3	46
14	Mesoproterozoic Tasmania: Witness to the East Antarctica–Laurentia connection within Nuna. Geology, 2015, 43, 759-762.	4.4	45
15	Successive hydration and dehydration of high-P mafic granofels involving clinopyroxene-kyanite symplectites, Mt Daniel, Fiordland, New Zealand. Journal of Metamorphic Geology, 2002, 20, 669-682.	3.4	43
16	Evidence for melt migration enhancing recrystallization of metastable assemblages in mafic lower crust, Fiordland, New Zealand. Journal of Metamorphic Geology, 2009, 27, 167-185.	3.4	42
17	A Multiproxy provenance approach to uncovering the assembly of East Gondwana in Antarctica. Geology, 2019, 47, 645-649.	4.4	41
18	Eastern Indian Ocean microcontinent formation driven by plate motion changes. Earth and Planetary Science Letters, 2016, 454, 203-212.	4.4	39

#	Article	IF	CITATIONS
19	Identifying Relic Igneous Garnet and Clinopyroxene in Eclogite and Granulite, Breaksea Orthogneiss, New Zealand. Journal of Petrology, 2013, 54, 1921-1938.	2.8	38
20	Hornblendite delineates zones of mass transfer through the lower crust. Scientific Reports, 2016, 6, 31369.	3.3	38
21	Direct observation of adakite melts generated in the lower continental crust, Fiordland, New Zealand. Terra Nova, 2005, 17, 73-79.	2.1	36
22	Exhumation of the Dayman dome metamorphic core complex, eastern Papua New Guinea. Journal of Metamorphic Geology, 2009, 27, 405-422.	3.4	36
23	Structural evolution of the Dayman dome metamorphic core complex, eastern Papua New Guinea. Bulletin of the Geological Society of America, 2011, 123, 2335-2351.	3.3	36
24	Cordillera Zealandia: A Mesozoic arc flare-up on the palaeo-Pacific Gondwana Margin. Scientific Reports, 2017, 7, 261.	3.3	36
25	Local partial melting of the lower crust triggered by hydration through melt–rock interaction: an example from Fiordland, New Zealand. Journal of Metamorphic Geology, 2017, 35, 213-230.	3.4	36
26	Tectonic cycles of the New England Orogen, eastern Australia: A Review. Australian Journal of Earth Sciences, 2019, 66, 459-496.	1.0	36
27	Roles for fluid and/or melt advection in forming high-P mafic migmatites, Fiordland, New Zealand. Journal of Metamorphic Geology, 2005, 23, 557-567.	3.4	34
28	Basin analysis in polymetamorphic terranes: An example from east Antarctica. Precambrian Research, 2013, 231, 78-97.	2.7	33
29	Thermomechanical evolution of the crust during convergence and deep crustal pluton emplacement in the Western Province of Fiordland, New Zealand. Tectonics, 2002, 21, 4-1-4-18.	2.8	32
30	Metastable persistence of pelitic metamorphic assemblages at the root of a Cretaceous magmatic arc – Fiordland, New Zealand. Journal of Metamorphic Geology, 2009, 27, 233-247.	3.4	32
31	Discovery of a microcontinent (Gulden Draak Knoll) offshore Western Australia: Implications for East Gondwana reconstructions. Gondwana Research, 2015, 28, 1019-1031.	6.0	32
32	Mass transfer in the lower crust: Evidence for incipient melt assisted flow along grain boundaries in the deep arc granulites of Fiordland, New Zealand. Geochemistry, Geophysics, Geosystems, 2016, 17, 3733-3753.	2.5	32
33	The recognition of former melt flux through highâ€strain zones. Journal of Metamorphic Geology, 2018, 36, 1049-1069.	3.4	30
34	The effect of preâ€ŧectonic reaction and annealing extent on behaviour during subsequent deformation: insights from paired shear zones in the lower crust of Fiordland, New Zealand. Journal of Metamorphic Geology, 2015, 33, 557-577.	3.4	29
35	Crustal Differentiation in a Thickened Arc—Evaluating Depth Dependences. Journal of Petrology, 2016, 57, 595-620.	2.8	29
36	The evolution of zircon during lowâ€ <i>P</i> partial melting of metapelitic rocks: theoretical predictions and a case study from Mt Stafford, central Australia. Journal of Metamorphic Geology, 2014, 32, 791-808.	3.4	28

#	Article	IF	CITATIONS
37	Complexity of In-situ zircon U–Pb–Hf isotope systematics during arc magma genesis at the roots of a Cretaceous arc, Fiordland, New Zealand. Lithos, 2016, 264, 296-314.	1.4	28
38	Patterns of strain localization in heterogeneous, polycrystalline rocks – a numerical perspective. Earth and Planetary Science Letters, 2017, 463, 253-265.	4.4	28
39	Granulite facies thermal aureoles and metastable amphibolite facies assemblages adjacent to the Western Fiordland Orthogneiss in southwest Fiordland, New Zealand. Journal of Metamorphic Geology, 2009, 27, 349-369.	3.4	27
40	The role of buoyancy in the fate of ultra-high-pressure eclogite. Scientific Reports, 2019, 9, 19925.	3.3	27
41	Mechanisms of melt extraction during lower crustal partial melting. Journal of Metamorphic Geology, 2021, 39, 57-75.	3.4	26
42	Virtual Petrographic Microscope: a multi-platform education and research software tool to analyse rock thin-sections . Australian Journal of Earth Sciences, 2014, 61, 631-637.	1.0	25
43	Melt-present shear zones enable intracontinental orogenesis. Geology, 2020, 48, 643-648.	4.4	25
44	Trace element partitioning during high-P partial melting and melt-rock interaction; an example from northern Fiordland, New Zealand. Journal of Metamorphic Geology, 2004, 22, 443-457.	3.4	24
45	Pinch and swell structures: evidence for strain localisation by brittle–viscous behaviour in the middle crust. Solid Earth, 2015, 6, 1045-1061.	2.8	24
46	Zircon Uâ€Pb Dating of a Lower Crustal Shear Zone: A Case Study From the Northern Sector of the Ivreaâ€Verbano Zone (Val Cannobina, Italy). Tectonics, 2018, 37, 322-342.	2.8	24
47	Symplectite formation in the presence of a reactive fluid: insights from hydrothermal experiments. Journal of Metamorphic Geology, 2017, 35, 281-299.	3.4	23
48	Chemical Signatures of Melt–Rock Interaction in the Root of a Magmatic Arc. Journal of Petrology, 2018, 59, 321-340.	2.8	23
49	Experimental alteration of monazite in granitic melt: Variable U–Th–Pb and REE mobility during melt-mediated coupled dissolution-precipitation. Chemical Geology, 2020, 544, 119602.	3.3	23
50	Tectonic drivers and the influence of the Kerguelen plume on seafloor spreading during formation of the early Indian Ocean. Gondwana Research, 2016, 35, 97-114.	6.0	22
51	The field and microstructural signatures of deformationâ€assisted melt transfer: Insights from magmatic arc lower crust, New Zealand. Journal of Metamorphic Geology, 2019, 37, 795-821.	3.4	21
52	Orthopyroxene–omphacite- and garnet–omphacite-bearing magmatic assemblages, Breaksea Orthogneiss, New Zealand: Oxidation state controlled by high-P oxide fractionation. Lithos, 2015, 216-217, 1-16.	1.4	20
53	Shape of pinch and swell structures as a viscosity indicator: Application to lower crustal polyphase rocks. Journal of Structural Geology, 2016, 88, 32-45.	2.3	19
54	Intracontinental Orogeny Enhanced by Farâ€Field Extension and Local Weak Crust. Tectonics, 2018, 37, 4421-4443.	2.8	19

#	Article	IF	CITATIONS
55	Fingerprinting Proterozoic Bedrock in Interior Wilkes Land, East Antarctica. Scientific Reports, 2019, 9, 10192.	3.3	19
56	Macquarie Island's Finch-Langdon fault: A ridge-transform inside-corner structure. Geology, 2003, 31, 661.	4.4	19
57	Evaluating the importance of metamorphism in the foundering of continental crust. Scientific Reports, 2017, 7, 13039.	3.3	18
58	Extension along the Australian-Pacific transpressional transform plate boundary near Macquarie Island. Geochemistry, Geophysics, Geosystems, 2003, 4, n/a-n/a.	2.5	17
59	Strike-slip tectonics during the Neoproterozoic–Cambrian assembly of East Gondwana: Evidence from a newly discovered microcontinent in the Indian Ocean (Batavia Knoll). Gondwana Research, 2017, 51, 137-148.	6.0	17
60	Enriching mantle melts within a dying mid-ocean spreading ridge: Insights from Hf-isotope and trace element patterns in detrital oceanic zircon. Lithos, 2011, 126, 355-368.	1.4	15
61	Retrograde metamorphism of the Wongwibinda Complex, New England Fold Belt and the implications of 2.5D subsurface geophysical structure for the metamorphic history. Australian Journal of Earth Sciences, 2010, 57, 357-375.	1.0	14
62	Petrogenesis and geochemical characterisation of ultramafic cumulate rocks from Hawes Head, Fiordland, New Zealand. New Zealand Journal of Geology, and Geophysics, 2012, 55, 361-374.	1.8	14
63	Vitriclastic lithofacies from Macquarie Island (Southern Ocean): compositional influence on abyssal eruption explosivity in a dying Miocene spreading ridge. Bulletin of Volcanology, 2010, 72, 165-183.	3.0	13
64	Anti lockwise <i>P–T</i> paths in the lower crust: an example from a kyaniteâ€bearing regional aureole, George Sound, New Zealand. Journal of Metamorphic Geology, 2010, 28, 77-96.	3.4	13
65	Geology and Age of Solander Volcano, Fiordland, New Zealand. Journal of Geology, 2013, 121, 475-487.	1.4	13
66	Tectonic implications of fault-scarp–derived volcaniclastic deposits on Macquarie Island: Sedimentation at a fossil ridge-transform intersection?. Bulletin of the Geological Society of America, 2005, 117, 18.	3.3	12
67	Inefficient high-temperature metamorphism in orthogneiss. American Mineralogist, 2019, 104, 17-30.	1.9	12
68	Sediment-Peridotite Reaction Controls Fore-Arc Metasomatism and Arc Magma Geochemical Signatures. Geosciences (Switzerland), 2021, 11, 372.	2.2	12
69	A detrital record of lower oceanic crust exhumation within a Miocene slow-spreading ridge: Macquarie Island, Southern Ocean. Bulletin of the Geological Society of America, 2011, 123, 255-273.	3.3	11
70	Microstructures reveal multistage melt present strain localisation in mid-ocean gabbros. Lithos, 2020, 366-367, 105572.	1.4	9
71	Glassy fragmental rocks of Macquarie Island (Southern Ocean): Mechanism of formation and deposition. Sedimentary Geology, 2009, 216, 91-103.	2.1	8
72	Mantle rocks in East Antarctica. Geological Society Memoir, 2023, 56, 17-32.	1.7	8

#	Article	IF	CITATIONS
73	Geochemical fingerprint of hyaloclasts in glassy fragmental rocks of Macquarie Island (Southern) Tj ETQq1 1 0.784		
	Journal of Earth Sciences, 2009, 56, 951-963.	1.0	7
74	High- <i>T</i> –low- <i>P</i> thermal anomalies superposed on biotite-grade rocks, Wongwibinda Metamorphic Complex, southern New England Orogen, Australia: heat advection by aqueous fluid?. Australian Journal of Earth Sciences, 2013, 60, 621-635.	1.0	7
75	The Keepit arc: provenance of sedimentary rocks in the central Tablelands Complex, southern New England Orogen, Australia, as recorded by detrital zircon. Australian Journal of Earth Sciences, 2017, 64, 401-418.	1.0	7
76	Provenance of Upper Jurassic–Lower Cretaceous strata in the Mentelle Basin, southwestern Australia, reveals a trans-Gondwanan fluvial pathway. Gondwana Research, 2021, 93, 128-141.	6.0	7
77	Interaction of Gravity Flows With a Rugged Mid-Ocean-Ridge Seafloor: An Outcrop Example from Macquarie Island. Journal of Sedimentary Research, 2011, 81, 355-375.	1.6	5
78	Metamorphism in the New England Orogen, eastern Australia: a review. Australian Journal of Earth Sciences, 2020, 67, 453-478.	1.0	5
79	10Be, 18O and radiogenic isotopic constraints on the origin of adakitic signatures: a case study from Solander and Little Solander Islands, New Zealand. Contributions To Mineralogy and Petrology, 2014, 168, 1.	3.1	4
80	Mesoproterozoic Tasmania: Witness to the East Antarctica-Laurentia connection within Nuna: REPLY. Geology, 2016, 44, e383-e383.	4.4	4
81	Determining relative bulk viscosity of kilometre-scale crustal units using field observations and numerical modelling. Tectonophysics, 2017, 721, 275-291.	2.2	4
82	Modelling the partial melting of metasediments in a low-pressure regional contact aureole: the effect of water and whole-rock composition. Geological Magazine, 2019, 156, 1400-1424.	1.5	4
83	Zircon U-Pb isotopic and geochemical study of metanorites from the chromite-mineralised Bacuri Mafic-Ultramafic Complex: Insights of a Paleoarchean crust in the Amapá Block, Guyana Shield, Brazil. Gondwana Research, 2022, 105, 262-289.	6.0	4
84	Oxide enrichment by syntectonic melt-rock interaction. Lithos, 2022, 414-415, 106617.	1.4	4
85	High-temperature–low-pressure metamorphism and the production of S-type granites of the Hillgrove Supersuite, southern New England Orogen, NSW, Australia. Australian Journal of Earth Sciences, 2018, 65, 191-207.	1.0	3
86	Ductile Deformation Without Localization: Insights From Numerical Modeling. Geochemistry, Geophysics, Geosystems, 2019, 20, 5710-5726.	2.5	3
87	Two belts of HTLP sub-regional metamorphism in the New England Orogen, eastern Australia: occurrence and characteristics exemplified by the Wongwibinda Metamorphic Complex. Australian Journal of Earth Sciences, 2020, 67, 479-507.	1.0	2
88	Oceanic Zircon Records Extreme Fractional Crystallization of MORB to Rhyolite on the Alarcon Rise Mid-Ocean Ridge. Journal of Petrology, 2022, 63, .	2.8	2